Volume 1 | Number 1 | Jan 2013 | Pages 1–100

Journal of
Materials Chemistry A

Materials for energy and sustainability
www.rsc.org/materialsA

Li⁺

ROYAL SOCIETY
OF CHEMISTRY

ROYAL SOCIETY
OF **CHEMISTRY**

www.rsc.org/materialsA

Journal Name

ARTICLE

New organic dyes based on dibenzofulvene bridge for highly efficient dye–sensitized solar cells.

Agostina Lina Capodilupo,[a] Luisa De Marco,[c] Eduardo Fabiano,[a,c] Roberto Giannuzzi, [c] Angela Scrascia,[a] Claudia Clarlucci,[a] Giuseppina Anna Corrente,[b] Maria Pia Cipolla,[c] Giuseppe Gigli[a,c,d] and Giuseppe Ciccarella[*a,e]

Three novel organic dyes, coded as **TK1**, **TK2** and **TK3,** respectively, incorporating two donor moieties, cyanoacrylic acid as acceptor/anchoring group, the dibenzofulvene core and an oligothiophene spacer in a 2D-π-A system, were designed, synthesized, and successfully utilized in dye-sensitized solar cells. The dye **TK3,** containing two thiophene rings, as spacer, shows an IPCE action spectrum with a high plateau from 390 nm to 600 nm, increased open-circuit photovoltage by 40 mV and short-circuit photocurrent by 7.03 mA cm^{-1}, respect to **TK1**. Using CDCA as the co-adsorbed material, the J_{sc} of **TK3** was increased to 14.98 mA cm^{-1} and a strong enhancement in overall conversion efficiency (7.45%) was realized by **TK3** compared to **TK1** (1.08%), in liquid electrolyte-based DSSCs.

Introduction

Dye-sensitized solar cells (DSSCs) have attracted a great deal of interest due to the potential of low cost production and the possibility to design new functional photoactive components to increase the solar-to-electrical energy conversion efficiency.[1] Compared with traditional silicon solar cells, DSSCs offer major advantages as low cost material, tunability of the absorption spectrum, and encouraging efficiency even under diffuse light. To date, DSSCs with validated efficiencies (η) record of > 11% have been obtained with ruthenium complexes[2] and porphyrin[3] dyes. Enormous efforts are also being dedicated to developing efficient dyes suitable for their modest cost, ease of synthesis and functionalization, large molar extinction molar coefficient and long-stability. Metal-free dyes or organic dyes meet all these criteria. Many different organic dyes with conversion efficiencies in the range of 6–8%[5a] have been reported in the last years but only a few examples have overcome efficiencies of 10%.[5]

However, despite the progress the optimization of the chemical structure of the organic components still needs further improvement. Most of the organic dyes used for highly efficient DSSCs have a long π-conjugated spacer between the donor (D) and acceptor (A) moieties. Nevertheless, the introduction of long π-conjugated segments gives prolonged rod-like molecules, which may facilitate the recombination of electrons with triiodide and magnify aggregation between molecules.[6] On

the basis of such findings, recently, organic dyes with a 2D−π−A structure, where two D moieties are connected to a π-spacer, were reported.[7] These studies suggested that organic dyes with the 2D−π−A structure may achieve better performance than the simple D−π−A structure.[8]

In this work, we present three novel sensitizers based on a 2D−π−A system, introducing the dibenzofulvene or fluorene-9-ylidene molecule as central core, labelled as **TK1**, **TK2** and **TK3** (Fig.1).

Fluorene derivatives have been intensively investigated as organic materials with advanced optical and electronic properties,[9] due to their unique properties, such as coplanarity, highly ordered π-stacked structures and high charge density. Nevertheless, to our knowledge, organic sensitizers based on special derivatives of fluorene, such as dibenzofulvene (**DBF**), so far have not been satisfactorily explored for applications in DSSCs.[10]

In our strategy, we investigate the trend of the power conversion efficiency of 3,6-diarylamino-substituted dibenzofulvene-based sensitizers with the addition of thiophene rings at the 9-ylidene position. Substitution at 3, 6 and 9 position of the fluorene, ensures an optimal π-conjugation through the fluorene skeleton, between the donor and acceptor units, making the compounds suitable for antenna-type systems in DSSC devices. We realized new 2D-π-A systems introducing two units of diphenylamine as donor groups[11] on the 3, 6-position of fluorene, and cyanoacrylic acid as acceptor group on

the 9-position of fluorene, in **TK1**, and on thiophene and bithiophene spacers, in **TK2** and **TK3,** respectively. This new architecture allowed us, in few steps and with good yields to obtain dyes with interesting device performances, achieving very promising PCE value of 7.45% with **TK3**.
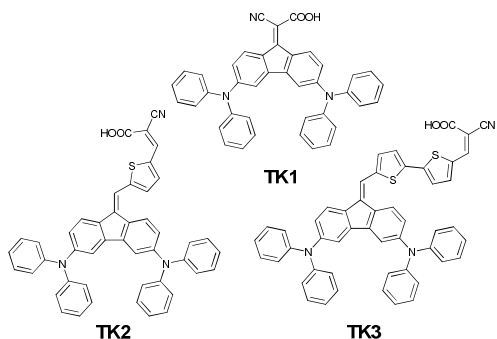

Fig. 1 Structure the dyes

Experimental

Materials and instrumentation

All reactions were carried out under a nitrogen atmosphere. Solvents were distilled freshly according to standard procedures. Commercial products were purchased from Sigma-Aldrich. ^{1}H and ^{13}C NMR spectra were recorded on a Bruker 400 MHz spectrometer. LC-MS spectra were acquired with an Agilent 6300 Series Ion Trap interfaced to an Agilent 1200 HPLC adopting the following general conditions: atmospheric pressure chemical ionization, positive ions, eluent chloroform, flow rate 0.200 mL min^{-1}, drying gas flow 5.0 L min^{-1}, nebulizer pressure 60 psi, drying gas temperature 350 °C, vaporizer temperature 325 °C, mass range 100–2200 m/z. UV-Vis absorption spectra were recorded on a Varian-Cary 500 spectrophotometer. Fluorescence spectra were obtained on a Varian Cary Eclipse spectro fluorimeter. The electrochemical characterization of the dyes was carried out by cyclic voltammetry (CV) using a AutoLab potentiostat (Methrom). A typical three-electrodes cell was assembled with a glassy carbon disk working electrode, a Pt-wire auxiliary electrode, and an Ag/AgCl non-aqueous reference electrode. Cyclic voltametries were acquired at 0.1 V s^{-1} scan rate on 1mM dye solutions prepared in the electrolyte solution which consisted of 0.1M tetrabutylammonium hexafluoroborate (TBAPF$_6$) in dichloromethane (CH$_2$Cl$_2$). All the solutions were previously degassed and N$_2$ atmosphere was kept in the cell. Ferrocene was added as an internal reference for calibration of the potential scale versus Fc$^+$/Fc couple. Potentials referred to ferrocene were then converted to Normal Hydrogen Electrode (NHE) by addition of 0.63 V.

Computational details

All calculations have been carried out with the TURBOMOLE[12] program package using the COSMO solvation model[13] Ground state calculations and geometry optimizations were performed using the BLOC functional.[14] Time-dependent calculations were carried out with the BHLYP functional.[15] In all calculations a def2-TZVP basis set[16] was employed. To quantify the charge-transfer character of each excited state two indicators were considered: the overlap indicator λ[17], which is computed as the spatial overlap between the occupied and unoccupied orbitals involved in the excitation; the electron displacement indicator Δr[18], which measures the distance between the ground-state and the excited-state charge distributions. We recall that small values of Λ (i.e. a small overlap between the occupied and unoccupied orbitals) indicate a greater charge-transfer character (when Λ = 0 an electron is completely transferred). On the contrary, Δr larger values indicate a more pronounced charge transfer character.

Fabrication of DSSCs and photovoltaic measurements

Fluorine-doped tin oxide (FTO, 15 Ω/sq, provided by Solaronix S.A.) glass plates were first cleaned in a detergent solution using an ultrasonic bath for 15 min, and then rinsed with water and ethanol. Double-layer electrodes (overall thickness 19 μm) were prepared as follows: a layer of commercial colloidal titania paste (Dyesol 18NR-T) was deposited onto the FTO glass and gradually heated in an oven in air to obtain a ~14 μm transparent nano-crystalline film; the temperature gradient was programmed as follows: 170°C (40 min), 350°C (15 min) and 430°C (30 min). This procedure was repeated for the scattering layer (5 μm) constituted by Solaronix D/SP colloidal paste. The double-layer electrode was eventually sintered at 450°C for 30 min. The thickness and the active area (0.16 cm^2) of the sintered photo-anodes was measured using a profilometer (Veeco Dektak 150 Surface Profiler). The dye loading was performed by keeping the electrodes for 14 h and under dark in 0.2 mM AcCN:CH$_2$Cl$_2$ = 1:0.01 v/v solutions of **TK1**, **TK2** and **TK3** containing, where needed, a known amount of chenodeoxycholic acid (CDCA). The counter-electrodes were prepared by sputtering a 50 nm Pt layer on a hole-drilled cleaned FTO plate. In a typical device construction procedure, the photo-anode and the counter-electrode were faced and assembled using a suitably cut 50 μm thick Surlyn® hot-melt gasket for sealing. The redox electrolyte (0.1 M LiI, 0.02 M I$_2$, 0.6 M 1-methyl-3-propylimidazolium iodide, and 0.5 M tert-butylpyridine in dry acetonitrile) was vacuum injected into the space between the electrodes through pre-drilled holes on the back of the counter electrode. The holes were eventually sealed using Surlyn® hot melt film and a cover glass. Photocurrent-voltage measurements were performed using a Keithley unit (Model 2400 Source Meter). A Newport AM 1.5 Solar Simulator (Model 91160A equipped with a 1000 W xenon arc lamp) serving as a light source. The light intensity (or radiant power) was calibrated to 100 mW cm^{-2} using as reference a Si solar cell. A mask with an aperture area of 0.25 cm2 was applied to the devices before measurements. The incident photon-to-current conversion efficiency (IPCE) was measured by the DC method using a computer-controlled xenon arc lamp (Newport, 140 W, 67005) coupled with a monochromator (Newport Cornerstone 260 Oriel 74125). The light intensity was measured by a calibrated silicon UV-photodetector (Oriel 71675) and the short circuit currents of the DSSCs were measured by using a dual channel optical power/energy meter, (Newport 2936-C). The surface concentrations (dye loading) of the dyes were assessed by spectrophotometric determination as follows: double layered photoanodes (14 + 5 μm, 1 cm^2) were sensitized with the same solutions used for devices; then the dyes were completely desorbed from the TiO$_2$ surface by immersing the substrates in a 0.01 M tetrabutylammonium hydroxide in DMF solution. The evaluation of the dye concentration in the solvent, obtained by UV-Vis measurements, allowed to estimate the amount of the adsorbed

molecules, expressed in terms of moles of dye anchored per projected unit area of the photoelectrode. Electrochemical impedance spectroscopy (EIS) was per-formed by an AUTOLAB PGSTAT 302N (Eco Chemie B.V.) in a frequency range between 100 kHz and 10 mHz. The impedance measurements were carried out at different voltage biases under 1.0 sun illumination. The resulting impedance spectra were fitted by using ZView (Scribner Associates) software.

Synthesis

3,6-dibromo-9H-fluoren-9-one (1) was synthesized following the literature procedure.[19]

3,6-bis(diphenylamino)-9H-fluoren-9-one (2). A mixture of 3,6-dibromo-9-fluorenone (0.400 g, 1.18 mmol), diphenylamine (0.440 g, 2.6 mmol) and sodium tert-buthoxide (0.288 g, 3 mmol) was added to suspension of $Pd(dba)_2$ (0.068 g, 0.120 mmol) and $PtBu_3$ (0.180 mL, 0.18 mmol, 1M in toluene) in anhydrous and deoxygenated toluene (5 mL), previous stirred under argon for 10 min. The resulting solution was heated under microwave irradiation at a constant temperature of 110°C for 50 min. The solvent was removed, and the residue was dissolved in dichloromethane and filtered off on short celite column. The solvent was removed by rotary evaporation, and the residue was purified by column chromatography (silica gel, 50:50 hexane, CH_2Cl_2) to give the product as an orange solid (0.424 g, 70%). ^{1}H-NMR (400 MHz, $CDCl_3$) δ 7.481 (d, $J = 8.18$ Hz, 2H) 7.29 (m, 8H) 7.11 (m, 12H) 7.02 (d, $J = 2$ Hz, 2H) 6.78 (dd, $J = 2$, 8.18 Hz, 2H); ^{13}C-NMR (100 MHz, $CDCl_3$) δ 190.7, 153.2, 146.5, 145, 129.4, 128.3, 125.4, 124.9, 124.2, 121.1, 113.1. MS (APCI) : calcd. for $C_{37}H_{26}N_2O$ 514,02; found: m/z = 515.10 [M+H]+.

2-(3,6-bis(diphenylamino)-9H-fluoren-9-ylidene)-2-cyanoacetic acid (TK1). $TiCl_4$ (0.560 mL, 5.13 mmol) dissolved in anhydrous $CHCl_3$ (1 mL) was slowly added into anhydrous THF (9 mL) under ice bath and nitrogen atmosphere. After stirring for 10 min, a mixture of compound **2** (0.1 g, 0.195 mmol) and cyanoacetic acid (0.198 g, 2.33 mmol) dissolved in THF (3 mL) were slowly added. After 10 min pyridine (0.75 mL) was added into the mixture and heated to reflux under Ar for 10 h. Then, the mixture was quenched with water and then extracted with dichloromethane. The combined organic phase was washed with sodium chloride and then dried on sodium sulfate. The solvent was removed by rotary evaporation and the crude residue was purified by column chromatography (silica gel, 100:10, CH_2Cl_2: methanol), to give the product a as dark powder (0.079 g, 70%). ^{1}H-NMR (400 MHz, $CDCl_3$); 6.68 (dd, 1H, $J = 2.3$ Hz, $J = 8.9$ Hz), 6.75 (dd, 1H, $J = 2.3$ Hz, $J = 8.8$ Hz), 6.95 (d, 1H, $J = 2.2$ Hz), 6.97 (d, 1H, $J = 2.2$ Hz), 7.11-7.15 (m, 12H), 7.28-7.32 (m, 8H), 8.27 (d, 1H, $J = 8.9$ Hz), 8.43 (d, 1H, $J = 8.8$ Hz);^{13}C-NMR (100 MHz, $CDCl_3$); 112.2, 120.2, 123.6, 123.7, 124.5, 124.6, 124.7, 124.9, 125.5, 125.7, 125.9, 126.0, 129.3, 129.4, 129.5, 141.3, 142.6, 143.5, 143.8, 146.0, 146.1, 146.8, 146.9, 150.9, 151.0, 152.1.MS (APCI) : calcd. for $C_{40}H_{27}N_3O_2$ 581.21; found: m/z = 582.17 [M+H]+.

N3,N3,N6,N6-tetraphenyl-9H-fluorene-3,6-diamine (3). To a suspension of aluminium chloride (0,156 g, 1.2 mmol) and borane-*tert*-butylamine (0.220 g, 2.52 mmol) in 2.5 mL of anhydrous dichloromethane at 0°C was added dropwise the compound 2 (0.200 g, 0.39 mmol) in 3 mL of dichloromethane. The final solution was allowed to warm to room temperature and stirred for 4 h before quenching with a solution of 0.1 M hydrochloric acid. The product was extracted with CH_2Cl_2, the combined organic layers were dried over sodium sulfate. The solvent was evaporated. The residue was purified by flash chromatography (silica gel: hexane/dichloromethane 9:1). Yielding 0.138 g (71%) of the product. ^{1}H-NMR (400 MHz, $CDCl_3$) δ 7.43 (dd, $J = 2.46$, 3.2 Hz, 4H), 7.20 (dd, $J = 7.34$, 7.36 Hz, 8H) 7.07 (d, $J = 7.54$ Hz, 8H) 7.03 (dd, $J = 2.02$, 2.02 Hz, 2H) 6.96 (t, $J = 7.3$ Hz, 4H) 3.86 (s, 2H); ^{13}C-NMR (100 MHz, $CDCl_3$) δ 147.93, 146.68, 142. 56, 138.93, 128.96, 125.57, 124.63, 123.28, 122.02, 117.09; MS (APCI) : calcd. for $C_{37}H_{28}N_2$ 500,23; found: m/z = 501,23 [M+H]+.

5-((3,6-bis(diphenylamino)-9H-fluoren-9-ylidene)methyl)thiophene-2-carbaldehyde (4). A mixture of potassium tert-buthoxide (0.050 g, 0.44 mmol), compound **3** (0.200 g, 0.4 mmol) and 2,5-thiophenecarbaldehyde (0.067 g, 0.48 mmol) was dissolved in 2 mL absolute ethanol. The resulting solution was heated under microwave irradiation at a constant temperature of 90°C for 20 min. The solvent was removed, and the residue was extracted with CH_2Cl_2. The solven was evaporated. The residue was purified by flash chromatography (silica gel: hexane/dichloromethane 1:1) to give the product as a red solid (0.175 g, 95%). ^{1}H-NMR (400 MHz, $CDCl_3$) δ 9.91 (s, 1H) 7.88 (d, $J = 8.53$ Hz, 1H), 7.73 (d, $J = 3.87$ Hz, 1H) 7.57 (d, $J = 8.33$, 1H) 7.44 (d, $J = 8.33$, 1H) 7.24 (m, 12H) 7.09 (d, $J = 7.58$ Hz, 8H) 7.02 (m, 4H) 6.96 (dd, $J = 2.06$, 8.33 Hz, 1H) 6.79 (dd, $J = 2.1$, 8.5 Hz); ^{13}C-NMR (100 MHz, $CDCl_3$) δ 182.3, 149.7, 149.1, 148.9, 147.4, 147.1, 143.3, 142.6, 140.1, 138.6, 136.3, 134.2, 130, 129.4, 129.2, 129.1, 125.3, 124.5, 124, 123.5, 123.2, 122.8, 122, 121.3, 115.3, 114.5, 113.6. MS (APCI): calcd. for $C_{43}H_{30}N_2OS$ 622,21; found: m/z = 623.36 [M+H]+.

3-(5-((3,6-bis(diphenylamino)-9H-fluoren-9-ylidene)methyl)thiophen-2-yl)-2-cyanoacrylic acid (TK2). A mixture of 5-((3,6-bis(diphenylamino)-9H-fluoren-9-ylidene)methyl)thiophene-2-carbaldehyde (0.1 g, 0.16 mmol) (**4**), cyanoacetic acid (0.017 g, 0.21 mmol), acetic acid (5 mL) and ammonium acetate (5 mg) was heated at 120°C for 12 h. The resulting red solution was poured into ice-cold water to produce a red precipitate. The solid was purified by flash chromatography (silica gel: methanol/dichloromethane 10:1) to give a as dark powder (0.082 g, 74%). ^{1}H-NMR (400 MHz, $CDCl_3$) δ 8.36 (s, 1H) 7.95 (d, $J = 8.51$ Hz, 1H) 7.81 (d, $J = 4.1$ Hz, 1H) 7.54 (m, 2H) 7.25 (m, 11H) 7.10 (d, $J = 8.31$ Hz, 8H) 7.04 (m, 4H) 6.95 (dd, $J = 2$, 8.3 Hz, 1H) 6.81 (dd, $J = 2$, 8.3 Hz, 1H); ^{13}C-NMR (100 MHz, $CDCl_3$) δ 151.6, 149.4, 149.1, 147.4, 147.1, 142.8, 140.2, 139.3, 138.5, 135.8, 134.2, 129.9, 129.8, 127.6, 125.3, 124.6, 124.1, 123.3, 122.9, 121.8, 121.4, 115.5, 115.2, 114.4, 113.8, 112.8, 112.5, 96.7. MS (APCI): calcd. for $C_{46}H_{31}N_3O_2S$ 689.21; found: m/z = 690.23 [M+H]+.

2,2'-bithiophene-5,5'-dicarbaldehyde (5). A mixture of $Pd(OAc)_2$ (0.180 g, 0.8 mmol) and diisopropylethylamine (2.8 mL, 16 mmol) was dissolved in anhydrous and deoxygenated toluene (6 mL). At this solution were introduced 5-bromothiophene-2-carbaldehyde (1.9 mL, 16 mmol) and tetrabutylammoniumbromide (2.578 g, 8 mmol). The resulting solution was deoxygenated for 15 min. and then heated to reflux for 5 h. The solvent was removed, and the residue was was purified by column chromatography (silica gel, 50:50 hexane, CH_2Cl_2) to give the product as a yellow solid (2.664 g, 75%) ^{1}H-NMR (400 MHz, $CDCl_3$) δ 9.9 (s, 2H) 7.73 (d, $J = 3.9$ Hz, 2H) 7.43 (d, $J = 3.9$ Hz, 2H); ^{13}C-NMR (100 MHz, $CDCl_3$) δ 182.31, 144.64, 143.71, 136.66, 126.24.

5'-((3,6-bis(diphenylamino)-9H-fluoren-9-ylidene)methyl)-[2,2'-bithiophene]-5-carbaldehyde (6). A mixture of potassium tert-buthoxide (0.050 g, 0.44 mmol), compound **3** (0.200 g, 0.4 mmol) and 2,2'-bithiophene-5,5'-dicarbaldehyde (0.105 g, 0.48 mmol) was dissolved in 2 mL

absolute ethanol. The resulting solution was heated under microwave irradiation at a constant temperature of 90°C for 20 min. The solvent was removed, and the residue was extracted with CH_2Cl_2. The solvent was evaporated. The residue was purified by flash chromatography (silica gel: hexane/dichloromethane 1:1) to give the product as a red solid (0.177 g, 63%). ^{1}H-NMR (400 MHz, $CDCl_3$) δ 9.87 (s, 1H) 8.1 (d, J = 8.54 Hz, 1H) 7.68 (d, J = 3.9 Hz, 1H) 7.58 (d, J = 8.3 Hz, 1H) 7.35 (s, 2H) 7.25 (m, 12H) 7.11 (d, J = 8.3 Hz, 8H) 7.03 (m, 6H) 6.86 (dd, J = 2, 8.5 Hz, 1H); ^{13}C-NMR (100 MHz, $CDCl_3$) δ 182.23, 148.67, 148.35, 147.51, 147.26, 146.56, 142.23, 141.57, 139.74, 137.15, 136.60, 136.41, 134.75, 130.46, 130.24, 129.15, 129.09, 126.34, 125.40, 125.11, 124.75, 124.38, 124.10, 123.88, 123.67, 123.05, 122.64, 122.24, 120.99, 115.59, 114.75, 114.43. MS (APCI) : calcd. $C_{47}H_{32}N_2OS_2$ 704.20; found: m/z = 705.16 $[M+H]^+$.

3-(5'-((3,6-bis(diphenylamino)-9H-fluoren-9-ylidene)methyl)-2,2'-bithiophen-5-yl)-2-cyanoacrylic acid acid (TK3). It was prepared in 70% yield from compound 6 by following a procedure similar to that described above for **TK2**. Red solid; ^{1}H-NMR (400 MHz, $CDCl_3$) 8.30 (s, 1H) 8.05 (d, J = 8.4 Hz, 1H) 7.70 (s, 1H) 7.56 (d, J = 8.9 Hz, 1H) 7.35 (d, J = 12 Hz, 2H) 7.24 (m, 12H) 7.10 (d, J = 8.5, 8H) 7.02 (m, 6H) 6.78 (d, J = 8.5 Hz, 2H); ^{13}C-NMR (100 MHz, $CDCl_3$) MS (APCI): calcd. for $C_{50}H_{33}N_3O_2S_2$ 771.20; found: m/z = 772.80 $[M+H]^+$.
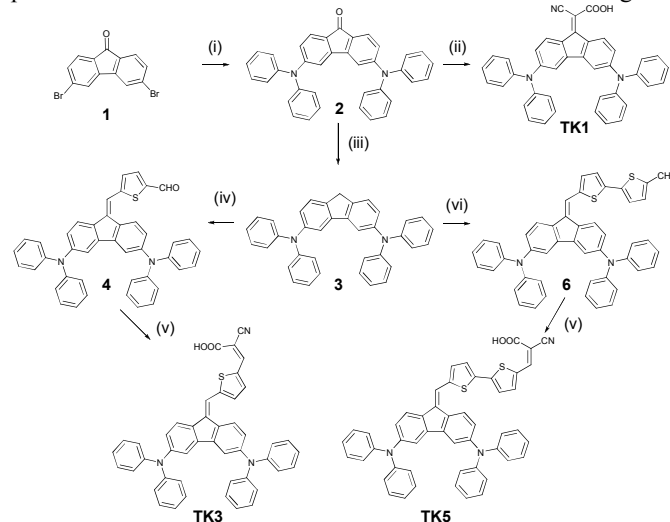
Results and discussion

Synthesis of the materials

The new dibenzofulvene-based (**TK**) organic dyes are shown in Fig.1, and the main synthetic patways are depicted in Scheme 1. Compound **2** was synthesized by a C-N cross-coupling reaction between the compound **1**[19] with 2.2 equivalents of diphenylamine, in the presence of Pd(dba)$_2$ (dba = dibenzylideneacetone) and P(tBu)$_3$,[20] in a microwave reactor. **TK1** was prepared *via* a Knoevenagel condensation of **2** with cyanoacetic acid, in the presence of TiCl$_4$.[21] The compound **3** was obtained by reduction reaction of the keto group of **2** by addition of borane-*tert*-butylamine and anhydrous AlCl$_3$. Then, the resulting product **3** was condensed with thiophene-2,5-dicarbaldehyde and 2,2'-bithiophene-5,5'-dicarbaldehyde (**5**) in the presence of KOtBu to obtain the compounds **4** and **6**, respectively. Finally, the organic dyes **TK2** and **TK3** were obtained *via* a Knoevenagel condensation of cyanoacetic acid with the aldehydes **4** and **6**, respectively, using ammonium acetate.

Photophysical properties

The UV-vis absorption spectra of the dyes in CH_2Cl_2 solution (ca. 10^{-5}M) are shown in Fig. 2. Absorption data are summarized in Table 1. As shown in Fig. 2, **TK1** displays the maximum absorption peaked at 449 nm. The incorporation of one thiophene ring as spacer between the **DBF** core and the acceptor units leads to sensitizer **TK2,** inducing a significant bathochromic shift of 73 nm, as well as an increased absorption intensity. The **TK3** is obtained by introduction of a second thiophene ring, its maximum absorption is centered at 485 nm and shows a significant increasing of the molar extinction coefficient (ε = 1.7 x 10^4 M^{-1}cm^{-1}).

The UV-vis absorption spectra of the dye-loaded TiO$_2$ films (~ 7 μm), shown Fig. 2 (right), display the same trend for the absorption maxima as those for the absorption in solution. **TK1**

displays a hypsochromically shifted absorption maxima (22 nm) in film on TiO$_2$ respect to the solution λ$_{max}$. This phenomenon has been observed for most of the organic

Scheme 1. Synthetic route to the sensitizers **TK1**, **TK2** and **TK3**. Reagents and conditions: (i) diphenylamine, Pd(dba)$_2$,P^{t}Bu$_3$, NaO^{t}Bu, Toluene, MW, 110°C, 50 min (ii) TiCl$_4$, pyridine, cyanoacrilic acid, THF (iii) AlCl$_3$, BH$_3$^{t}BuNH$_2$ complex, CH$_2$Cl$_2$, (iv) 2,5-thiophenecarbaldehyde, KO^{t}Bu, EtOH, MW, 100°C, 5 min, (v) NH$_4$AcO, CH$_3$COOH, 120°C, 3h, (vi) 2,2'-bithiophene-5,5'-dicarbaldehyde (**5**), KO^{t}Bu, EtOH, MW 100°C, 5 min

sensitizers and it is due to the deprotonation of cyanoacrylic acid group.[22]

On the other hand, upon adsorption onto nanocrystalline TiO$_2$ surface, a small (~ 5 nm) or negligible shift in the absorption maximum can be observed for **TK3** and **TK2**, respectively. At the same time, a beneficial broadening of the absorption bands improves light-harvesting and a short-circuit current enhancement is also expected.
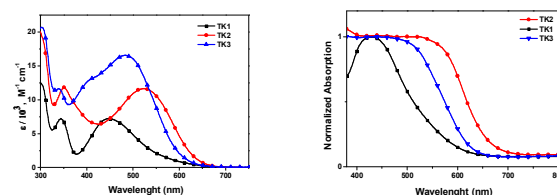

Fig. 2. Absorption dyes in CH_2Cl_2 solution (left) and on TiO$_2$ (right).

Electrochemical properties

The cyclic voltammograms of the dyes are shown in the Supporting Information (Fig S1) and the relevant electrochemical data are presented in Table 1. The first oxidation potentials, corresponding to the HOMO energy levels of the **TK,** were determined to be 4.99, -5.08 and -5.35, respectively for **TK3**, **TK2** and **TK1**. These values corresponded to 0.94, 1.03 and 1.29 *vs*. NHE, respectively, which are more positive than the redox potential of the I$^-$/I$_3^-$ redox couple (0.4 V *vs*. NHE), indicating that reduction of the oxided dyes whit I$^-$ ions is thermodynamically feasible. The excited state (E$^*_{0-0}$) of the sensitizer was estimated from the

difference between the first oxidation potential and the zero - zero excitation energy (E_{0-0}) derived from the absorption onset. The more negative excited state oxidation potential of **TK** dyes (E^*_{0-0}, -0.89 to -1.14 V *vs.* NHE) than the conduction band-edge

Table 1 Absorption and electrochemical parameters of the dye

Dyes	λ_{abs} ($\varepsilon \times 10^3 M^{-1}cm^{-1}$)[a] (nm)	λ_{abs} [b] (nm)	E_{ox}[c](V)	HOMO/LUMO (eV)	E_{0-0}[d](eV)	E^*_{ox}[e](V)
TK1	449 (7.3)	427	1.29	-5.35/-3.17	2.18	-0.89
TK2	522 (12)	-*	1.03	-5.08/-3.13	1.96	-0.93
TK3	485 (17)	-	0.94	-4.99/-2.91	2.08	-1.14

[a]Absorption maximum in dichloromethane (~10-5 M) solution. [b] Absorption maximum on TiO$_2$ film. [c] Oxidation potential in CH$_2$Cl$_2$ solution containing 0.1 M of tetrabutylammonium hexafluorophosphate with a scan rate of 100 mVs-1 (*vs.* NHE) and calibrated against ferrocene. [d] The bandgap, E_{0-0} was determined from onset of absorption spectrum. [e] $E^*_{ox} = E_{ox} - E_{0-0}$. * The peaks of **TK2** and **TK3** are difficult to determine.

level of the TiO$_2$ elecrode (-0.5 vs. NHE),[23] ensures the electron injection into the conduction band of TiO$_2$.

Theoretical approach

To further study the electronic and optical properties of the dyes we performed density functional theory (DFT) and time-dependent (TD) DFT calculations. The TD-DFT results are in good agreement with the experimental spectra and show that the broad absorption bands observed in solution in fact consist of several singlet excitations. (Tab. 2 and Fig. 3). All the excitations are described by single-particle transitions from the lowest occupied orbitals to the higher unoccupied molecular orbital (LUMO) and have a substantial charge-transfer character. This fact is indicated by the inspection of the orbitals' isodensity plots (Fig. 4) as well from the values of the indicators Λ[17] and Δr.[18] In particular, the latter shows that the photoinduced charge separation increases consistently in the series **TK1-TK2-TK3** (Δr = 2.39, 5.12, and 5.95 Å respectively), indicating the positive effect of thiophene insertion in the spacer.

The inclusion of thiophene units was also found to have an effect on the ionization potential and electron affinity, causing a reduction of the former and an increase of the latter (Tab. 3), possibly because of the induced increase of π conjugation. We remark that this finding correlates well with the computed reduction in the optical gap going from **TK1** to **TK3**. Furthermore, the trend was confirmed by cyclic voltammetry (CV) measurements (see Table 1 and Fig S1 in ESI).

Table 2 Excitation energies and absorption spectra

System	Energy (eV)	o.s.	transitions	λ	Δr (Å)	fit exp.
TK1	2.32	0.22	H→L (86%)	0.54	2.78	2.47
			H-2→L (10%)			
	2.88	0.77	H-1→L (94%)	0.67	2.28	2.79
TK2	2.28	0.35	H→L (87%)	0.63	4.73	2.38
			H-2→L (7%)			
	2.49	0.13	H-1→L (84%)	0.39	6.15	2.90
			H-3→L (5%)			
TK3	2.14	0.46	H→L (84%)	0.62	6.05	2.51
			H-2→L (9%)			
	2.66	0.11	H-1→L (78%)	0.30	8.65	3.02
			H-1→L+1 (13%)			
	3.21	0.26	H-2→L (63%)	0.67	4.62	3.20
			H→L+1 (20%)			

TD-DFT excitation energies (eV), oscillator strengths, main single-particle transitions, overlap indicator Λ, and electron displacement indicator Δr, for the lowest-lying singlet excitations of **TK1**, **TK2**, and **TK3**. The last column of the table reports excitation energies obtained by fitting the experimental spectra with Gaussian functions.

Table 3. Ionization potential (IP) and electron affinity (EA) of the **TK1**, **TK2**, **TK3** dyes in eV calculated with DFT. Both quantities were obtained as energy differences between the neutral dye and the anion/cation.

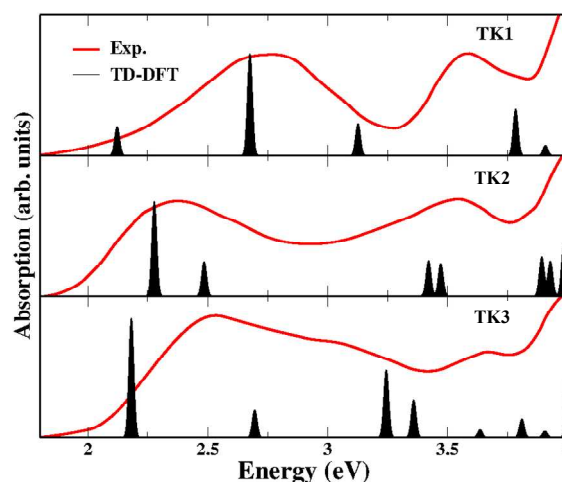|	TK1	TK2	TK3
IP	6.12	5.93	5.75
EA	1.74	2.03	2.19

Fig. 3. Comparison of the experimental and TD-DFT absorption spectra of **TK1**, **TK2**, and **TK3** dyes.
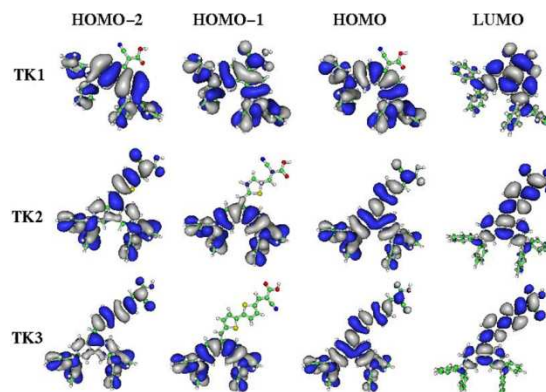

Fig. 4. Isodensity plots of the most relevant frontier orbitals of the dyes.

Photovoltaic devices

The performances of the new sensitizers were investigated by constructing test devices. The photovoltaic parameters in terms of short circuit current (J_{sc}), open circuit voltage (V_{oc}), fill factor (FF), and the resulting power conversion efficiency (η) are summarized in Table 4. While, the photocurrent–voltage (J–V) curves are plotted in Fig. 5.

The power conversion efficiencies of the devices based on **TK1**, **TK2** and **TK3** dyes are 2.1%, 5.0% and 5.4%, respectively. This enhancement is mainly attributed to an increase in J_{sc}, from 4.52 mA/cm^2 of the **TK1** dye to 10.85 and 11.55 mA/cm^2 achieved with the **TK2** and **TK3** dyes, respectively. The IPCE spectra, shown in Fig. 5, partially explain what happens: the **TK1**-based device presents the lower photoresponse showing a maximum of ~20% at 430 nm compared to the plateau of ~50% in the 450-550 nm region obtained for the **TK2** and **TK3**-based devices, in good accordance with the absorption spectra.

An estimation of the dye loading for **TK1**, **TK2** and **TK3** revealed that the amount of adsorbed **TK1** is lower compared to **TK2** and **TK3**. The bulkier molecular structure of TK1 reasonably hampers the access to adsorption sites with respect to the **TK2** and **TK3** sensitizers, providing an explanation for the lower efficiencies, ascribable to the increased probability of detrimental charge recombination processes.

To further investigate the relationship between the molecular structure and photovoltaic performance, the capacitance (C_{meas}, Fig. 6), the charge transfer resistance at the TiO$_2$/dye/electrolyte interface (R_{ct}, Fig. 6) and the electron lifetime (Fig. 7) were measured by electrochemical impedance spectroscopy (EIS). Since all devices were fabricated and tested in the same conditions, only the differences in the molecular structure of the sensitizers influenced the electrochemical parameters.

Table 4 Photovoltaic parameters for DSSCs based on **TK1**, **TK3** and **TK5** dyes.

Dye	CDCA[a] [mM]	η/%	FF	V_{OC} (V)	J_{SC} (mA cm^{-2})	Dye loading (10^{-7}mol/cm^2)
TK1	0	2.14	0.75	0.63	4.52	2.1
	10	1.08	0.70	0.70	2.21	1.5
TK2	0	5.01	0.70	0.66	10.85	2.5
	10	4.72	0.73	0.73	8.85	1.8
TK3	0	5.42	0.70	0.67	11.55	2.6
	10	7.45	0.71	0.70	14.98	2.0
N719	0	8.11	0.70	0.79	14.68	1.7

a CDCA = chenodeoxycholic acid

The lower R$_{ct}$ was found for the **TK1**-based device indicating that injected electrons are easily subjected to recombination with the oxidized form of the sensitizer or with the redox species present in the electrolyte. The extension of the π-bridge through the introduction of one or two thienyl moieties was helpful to increase the interfacial resistance, as also indicated by the higher V_{oc} (Table 4), suggesting that a larger amount of photo-generated electrons can reach the contact, justifying the higher photocurrent.

The apparent electron lifetime (Fig 7) of **TK1** is remarkably shorter than those of **TK2** and **TK3** dyes, which further confirms that injected electrons from **TK1** undergo to an easier recombination.

Due to the high planarity of the sensitizers, favored by the presence of the **DBF** core, a fast intramolecular charge

transfer is expected as well as an unfavourable π-π stacking which may lead to recombination phenomena. For this reason the use of CDCA as co-adsorbent was implemented.

The performances of the CDCA co-sensitized devices yielded 1.1%, 4.72% and 7.45% efficiencies for **TK1**, **TK2** and **TK3** dye, respectively showing a remarkable improvement for the **TK3** dye.
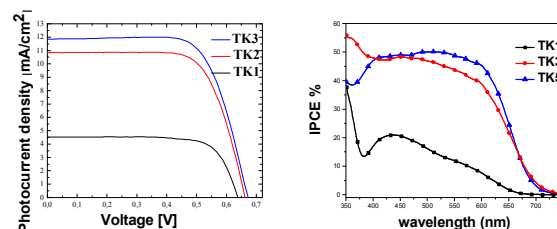

Fig. 5 *J-V* curves of DSSCs based on the dyes, without CDCA co-sensitization (left). IPCE spectra of DSSCs based on the dyes, without CDCA co-sensitization (right).
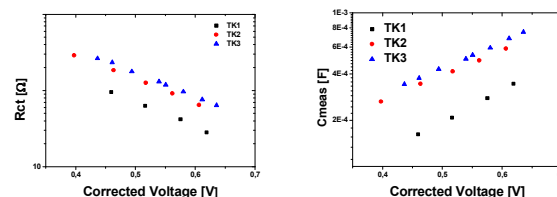

Fig. 6. Measured capacitance as a function of the corrected potential (left). Charge transfer resistance as a function of the corrected potential (right)
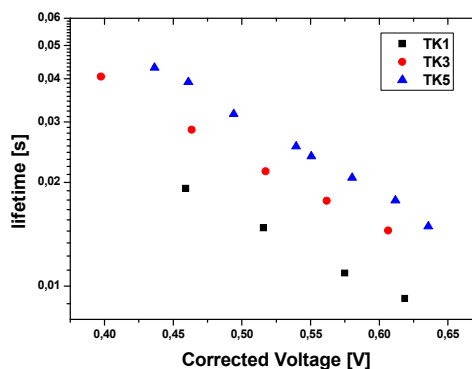

Fig. 7. Apparent electron lifetime as a function of the corrected potential.

These results could be explained considering that the co-adsorbent CDCA minimizes the detrimental dye aggregation of planar sensitizers but reduces the dye up-take by competing with the dye for the binding at the TiO$_2$ surface.

In the case of the **TK1** dye, due to their higher steric hindrance, the CDCA lowers the performances of the device because unfavorably competes with the sensitizer. On the other hand, for the **TK3** dye, the lowering of the dye coverage is well counterbalanced by the reduction of the π-π stacking and thus of the intermolecular quenching, leading

to the higher photovoltaic performances (η = 7.45%, FF = 0.71, V_{oc} = 0.70 V, J_{sc} = 14.98 mA/cm^2). (Fig. 8)
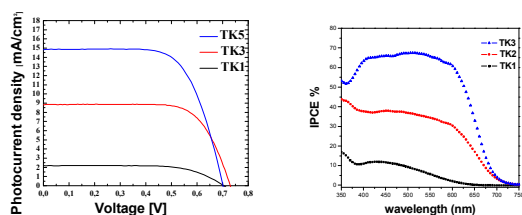

Fig. 8. J-V curves of **TK** dyes/CDCA DSSCs based on the co-adsorbed approach (left). IPCE spectra of DSSCs based on the dyes with co-adsorbed CDCA.

Conclusions

In summary, three novel dibenzofulvene-centered sensitizers (**TK1**, **TK2** and **TK3**) with different thiophene units have been designed and successfully synthesized. The molecular design strategy here can effectively improve the efficiency of solar conversion which is generally determined by light harvesting efficiency, electron injection efficiency, and reduction of the charge recombination phenomena. DSSCs using these sensitizers exhibited efficiencies of 2.14-5.42% under AM 1.5 illumination. Upon adding CDCA as a co-adsorbed, an energy conversion efficiency as high as 7.45% was achieved with **TK3** dye.

Our further research on broadening the absorption spectra to infrared region through molecular engineering or co-sensitization is under study.

Acknowledgements

Notes and references

^{a} Istituto Nanoscienze – CNR, National Nanotechnology Laboratory (NNL), Via Arnesano, 73100 Lecce, Italy.

^{b} Università della Calabria, via Pietro Bucci, 87036 Arcavacata di Rende, Cosenza, Italy

^{c} Center for Biomolecular Nanotechnologies (CBN) Fondazione Istituto Italiano di Tecnologia (IIT), Via Barsanti 1, Arnesano, 73010, Italy

^{d} Dipartimento di Matematica e Fisica "Ennio De Giorgi", Università del Salento, Via Monteroni, 73100, Lecce, Italy.

^{e} Dipartimento di Ingegneria dell'Innovazione, Università del Salento, Via Monteroni, 73100, Lecce, Italy.Address here.

1   (a) P. Qin, X. Yang, R. Chen, L. Sun, T. Marinado, T. Edvinsson, G. Boschloo and A. Hagfeldt, *J. Phys. Chem. C*, 2007, **111**, 1853-1860. (b) B. O'Regan and M. Gratzel, *Nature*, 1991, **353**, 737-740. c) M. K. Nazeeruddin, A. Kay, I. Rodicio, R. Humphry-Baker, E. Mueller, P. Liska, N. Vlachopoulos and M. Graetzel, *J. Am. Chem. Soc.*, 1993, **115**, 6382-6390.

2   (a) M. K. Nazeeruddin, F. De Angelis, S. Fantacci, A. Selloni, G. Viscardi, P. Liska, S. Ito, B. Takeru and M. Grätzel, *J. Am.Chem. Soc.*, 2005, **127**, 16835; (b) C. Chen, M. Wang, J. Li, N. Pootrakulchote, L. Alibabaei, C. Ngoc-le, J. Decoppet, J. Tsai, C. Grätzel, C. Wu, S. M.Zakeeruddin and M. Grätzel, *ACS Nano*, 2009, **3**, 3103. c) Y. Chiba, A. Islam, Y. Watanabe, R. Komiya, N. Koide and L. Y. Han, *Jpn. J. Appl. Phys., Part 2*, 2006, **45**, L638. d) F. Gao, Y. Wang, D. Shi, J. Zhang, M. Wang, X. Jing, R. Humphry-Baker, P. Wang, S. M. Zakeeruddin and M., *J. Am. Chem. Soc.*, 2008, **130**, 10720.

3   (a) J. Yina, M. Velayudham, D. Bhattacharya, H. Lin and K. Lu, *Coord. Chem. Rev.*, 2012, **256**, 3008; (b) J. Clifford, M. Planells and E. Palomares, *J. Mater. Chem.*, 2012, **22**, 24195; (c) L. Li and E. W. Diau, *Chem. Soc. Rev.*, 2013, **42**, 291; (d) M. Liang and J. Chen, *Chem. Soc. Rev.*, 2013, **42**, 3453. (e) S.Mathew, A. Yella, P. Gao, R. Humphry-Baker, B. F. E. Curchod, N. Ashari-Astani, I. Tavernelli, U. Rothlisberger, Md. K. Nazeeruddin and M. Grätzel, *Nat. Chem.*, 2014, **6**, 242.

4   (a) S. Cai, X. Hu, Z. Zhang, J. Su, X. Li, A. islam, L. Han and H. Tian, *J. Mater. Chem. A*, 2013, 1, 4763. (b) H. Chen, H. Huang, X. Huang, J. N. Clifford, A. Forneli, E. Palomares, X. Zheng, L Zheng, X Wang and P Shen, *J. Phys. Chem. C*, 2010, **114**, 3280. (c) G. Li, K.-J Jiang, Y.-F Li, S.-L Li, L.-M Yang,. *J. Phys. Chem. C*, 2008, **112**, 11591. (d) L.-Y Lin, C.-H Tsai,. K.-T Wong, T.-W Huang, L. Hsieh, S.-H Liu., H.-W Lin, C.-C. Wu, S.-H Chou and S.-H Chen, *J. Org. Chem.*, 2010, **75**, 4778.

5   (a) S. Ahmad, E. Guillen, L. Kavan, M. Grätzel and Md. K. Nazeeruddin, *Energy Environ. Sci*., 2013, **6**, 3439. (b) A Mishra, M. K. R. Fischer and P.Bauerle, *Angew. Chem. Int. Ed.*, 2009, **48**, 2474. (c). J.-H Yum et al. *Sci. Rep.*, 2013, **3**, 2446. (d) M Zhang,. et al. *Energy Environ. Sci.*, 2013, **6**, 2944. (e) Y. Wu and W Zhou, *Chem. Soc. Rev.*, 2013, **42**, 2039. (f) W. Zeng et al, *Chem Mater.*, 2010, **22**, 1915. (g) D. Joly, L. Pelleia, S. Narbey, F. Oswald, J. Chiron, J. N. Clifford, E. Palomares and R. Demadrille, *Sci. Rep.*, 2014, **4**, 4033.

6   (a) R. F Fink, J. Seibt, V. Engel, M. Renz, M Kaupp, S Lochbrunner, H.-M Zhao, J. Pfister, F. Würthner and B. Engels, *J. Am. Chem. Soc.*, 2008, **130**, 12858. (b) A. Ehret, L.Stuhl, M. T. Spitler, *J. Phys. Chem. B*, 2001, **105**, 9960. (c) M. C Gather, D. D. C. and Bradley, *Adv. Funct. Mater.* 2007, **17**, 479. (d) K. Sayama, K Hara. N Mori, M. Satsuki, S Suga, S.Tsukagoshi, Y. Abe, H Sugihara and H. Arakawa, *Chem. Commun.*, 2000, 1173.

7   (a) H Chen, H Huang, X. Huang, J. N Clifford, A. Forneli, E. Palomares, X. Zheng, L Zheng, X. Wang, P Shen, *J. Phys. Chem. C*, 2010, **114**, 3280. (b) K. Tang, M Liang, Y. K Liu, Z Sun, S Xue,. *Chin. J. Chem.*, 2011, **29**, 89. (c) C.-H Yang, S.-H. Liao, Y.-K Sun, Y.-Y.Chuang,; T.-L. Wang, Y.-T. Shieh, and W.-C. Lin, *J. Phys. Chem. C*, 2010, **114**, 21786. (d) T. Daeneke, T.-H. Kwon, A. B. Holmes, N. W Duffy, U Bach and. L.Spiccia, *Nat. Chem.* 2011, **3**, 211. (e) Z Ning and H.Tian, *Chem. Commun.*, 2009, 5483.

8   (a) A. Abbotto, N. Manfredi, C. Marinzi, F. De Angelis, E. Mosconi, J.-H. Yum, X. Zhang, Md. K. Nazeeruddin and M. Grätzel, *Energy Environ. Sci.*, 2009, **2**, 1094. (b) M. K. R. Fischer, S. wenger, M. Wang, A. Mishra, S. M. Nazeeruddin, M. Grätzel and P. Bauerle, *Chem. Mater.*, 2010, **22**, 1836.

9   (a) Y. Wu and W. Zhu, *Chem. Soc. Rev.*, 2013, 42, 3453. (b) D. Neher, *Macromol. Rapid Commun.*, 2001, **22**, 1365. (c) R. Abbel, A. P. H. J. Schenning and E. W. Meijer, *J. Pol. Sci. Part A: Pol. Chem.*, 2009, **47**, 4215.(d)W. Li, Y. Wu, X. Li, Y. Xie and W. Zhu, *Energy & Environ. Sci.*, 2011, **4**, 1830. (e) S. Higashijima, Y. Inoue, H. Miura, Y. Kubota, K. Funabiki, T. Yoshida and M. Matsui, *RSC Advances*, 2012, **2**, 2721. (f) G. Marzari, J. Durantini, D. Minudri, M. Gervaldo, L. Otero, F. Fungo, G. Pozzi, M. Cavazzini, S. Orlandi and S. Quici, *J. Phys. Chem. C*, 2012, **116**, 21190. (g) H. Kong, D. H. Lee, I.-N. Kang, E. Lim, Y. K. Jung, J.-H. Park, T. Ahn, M. H. Yi, C. E. Park and H.-K. Shim, *J. Mat. Chem.*, 2008, **18**, 1895. (h) M. Surin, P. Sonar, A. C. Grimsdale, K. Mullen, S. De Feyter, S. Habuchi, S. Sarzi, E. Braeken, A. Ver Heyen, M. Van der Auweraer, F. C. De Schryver, M. Cavallini, J.-F. Moulin, F. Biscarini, C. Femoni, R. Lazzaroni and P. Leclere, *J. Mat. Chem.*, 2007, **17**, 728.

10 (a) L. Morena, M. Gervaldo, F. Fungo, L. Otero, T. Dittrich, C.-Y. Lin, L.-C. Chi, F.-C. Fang, S.-W. Lii, K.-T. Wong, C.-H. Tsai and C.-C. Wu, *RSC Advances*, 2012, **2**, 4869. (b) Y. Numata, A. Islam, H. Chen and L. Y. Han, *Energy Environ. Sci.*, 2012, **5**, 8548.

11 (a) A. Scrascia, L. De Marco, S. Laricchia, R. A. Picca, C. Carlucci, E. Fabiano, A. L. Capodilupo, F. Della Sala, G. Gigli and Giuseppe Ciccarella, *J. Mater. Chem. A*, 2013, **1**, 11909; (b) A. Scrascia, M. Pastore, L. Yin, R. A. Picca, M. Manca, Y.-C. Guo, F. De Angelis, F. Della Sala, R. Cingolani, G. Gigli and Giuseppe Ciccarella, *Current Organic Chemistry*, 2011, **19**, 3535.

12 TURBOMOLE V6.4 2012, a development of University of Karlsruhe and Forschungszentrum Karlsruhe GmbH, 1989–2007, TURBOMOLE GmbH, since 2007; available from http://www.turbomole.com.

13 (a) A. Klamt and G. Schuurman, *J. Chem. Soc., Perkin Trans.*, 1993, **2**, 799.; (b) A. Klamt and V. Jonas, *J. Chem. Phys.*, 1996, **105**, 9972.

14 (a) L. A. Constantin, E. Fabiano and F. Della Sala, *J. Chem. Theory Comput.*, 2013, **9**, 2256.; (b) L. A. Constantin, E. Fabiano and F. Della Sala, *Phys. Rev. B*, 2012, 86, 035130.

15 A. D. Becke, *J. Chem. Phys.*, 1993, **98**, 1372.

16 F. Weigend, M. Haser, H. Patzelt and R. Ahlrichs, *Chem. Phys. Lett.*, 1998, **294**, 143.

17 M. J. G. Peach, P. Benfield, T. Helgaker and D. J. Tozer, *J. Chem. Phys.*, 2008, 128, 044118.

18 C. A. Guido, P. Cortona, B. Mennucci, and C. Adamo, *J. Chem. Theory Comput.*, 2013, **9**, 3118.

19 B. Kobin, L. Grubert, S. Blumstengel, F. Henneberger and S. Hecht, *J. Mater. Chem.*, 2012, **22**, 4383.

20 S. A. Odon, K. Lancaster, L. Beverina, K. M. Lefler, N. J. Thompson, V. Coropceanu, J.-L. Bredas, S. R. Marder and S. Barlow, *Chem. Eur. J.*, 2007, **13**, 9637.

21 L. Marcor, M. Gervaldo, F. Fungo, L. Otero, T. Dittrich, C-Y. Lin, L-C. Chi, F. C. Fang, S.-W. K.-T. Wong, C.-H. Tsai and C.-C Wu, *RSC Adv.*, 2012, **2**, 4869.

22 H. Tian, X. Yang, R. Chen, R. Zhang, A. Hagfeldt and L. Sun, *J. Phys. Chem. C*, 2008, **112**, 11023.

23 A. Hagfeldt, G. Boscholoo, L. Sun, L. Kloo and H. Pettersson, *Chem Rev.*, 2010, **110**, 6595.

We demonstrate that a carbon-bridged dibenzofulvene (DBF)-linked dye serves as a novel and efficient architecture for dye-sensitized solar cell. The DSSC based on **TK3** containing two thiophene ring between the DBF and acceptor group displays a maximum power conversion efficiency of 7.45%, high open circuit voltages reaching close to 0.70 V and based on the iodide/triiodide electrolyte.